Assessment of Low-Cost Infrared Thermography Systems for Medical Screening in Nursing Homes

Bruno Braga*, Gabriel Queirós*, Carlos Abreu*, Sérgio Ivan Lopes*[†‡]

* ADiT-LAB, Instituto Politécnico de Viana do Castelo, 4900-348 Viana do Castelo, Portugal

[†] IT - Instituto de Telecomunicações, Campus Universitário de Santiago, 3810-193 Aveiro, Portugal

[‡] Corresponding Author: sil@estg.ipvc.pt

Abstract—Recent developments in microbolometer array technology have favored the spread of low-cost infrared cameras and their dissemination in different application domains, in particular, regarding medical applications. According to the World Health Organization, elevated body temperature is one of the most common indicators of an abnormal medical condition. Indeed, body temperature monitoring is paramount, particularly in pandemic scenarios like the world is living in since late 2019. In this context, we aim to develop a body temperature screening system using a low-cost infrared thermography system designed to be used in nursing homes. Towards our goal, this work presents the assessment procedure and the results obtained when comparing the performance of two low-cost infrared cameras with a more expensive flagship device.

Index Terms—Infrared Thermography, Low-Cost Infrared Cameras, Nursing Homes

I. Introduction

Thermography has experienced notable advances in the last decades. Such developments, in particular the use of microelectromechanical technologies for manufacturing larger 2D microbolometers arrays, have contributed to increasing the sensor's sensitivity allowing to obtain better images at a lower price. Such advances have allowed the massification of thermography across different application fields, being the thermal medical imaging one of the most relevant [1], [2].

Due to its non-invasive nature, thermal imaging has raised notoriety in the medical community. It has been used in the assessment of several diseases such as diabetic neuropathy [3], rheumatoid arthritis [4], orthopedic surgery [5] and also in animal disease detection [6]. In this work, we are interested to detect abnormal body temperature that can be associated with several medical conditions, e.g., infection, inflammation, or ischemia. Additionally, due to the pandemic scenario, we are living in since late 2019, body temperature monitoring has become extremely important to identify possible infections by the SARS-CoV-2 virus, especially regarding the groups at risk, such as the elderly. Moreover, using thermography allows screening people for possible SARS-CoV-2 infections without contact and at a safe distance. In this context, we intend to develop a body temperature screening system using low-cost thermographic technology, designed taking into account the specific requirements of nursing homes. Towards our goal, this work presents the assessment procedure and the results obtained when comparing the performance of two low-cost infrared cameras (i.e., the Melexis MLX90640 and the Lepton 2.5) with a more expensive flagship device (i.e., the FLIR E54).

The remainder of this paper is organized as follows, Section II surveys some relevant works, focusing on those using low-cost thermographic technology for body temperature monitoring. Section III provides detailed information about the procedure used to assess the low-cost infrared cameras. Section IV presents the results obtained. Finally, Section V presents the conclusions and the future work.

II. Related Work

The spread of pathogenic microorganisms such as bacteria, parasites, fungi, or viruses is the cause of several infectious diseases among people. Indeed, viruses and bacteria are associated with the most relevant pandemics throughout the last centuries. Currently, the worldwide outbreak of COVID-19, caused by the fast spread of the SARS-CoV-2 virus, represents a significant threat to world health. Aiming to contain the spread of COVID-19 several strategies have been proposed, including the use of infrared thermography to early fever screening. Although fever is not the only symptom of COVID-19[1], 88% of people who had a positive diagnosis

---

[1]N.B., to have a positive COVID-19 diagnosis it's necessary to perform a laboratory analysis, usually a PCR test.

for COVID-19 reported to had a fever. For this reason, fever screening is widely used in public environments as a measure to mitigate the spread of this disease [7].

During the H1N1 influenza pandemic in 2009, Hewlett *et al.* [8] evaluate an infrared thermal detection system for fever screening in a clinical setting. They reported that the technology was able to screen out individuals without fever and have a high positive likelihood ratio, indicating that those screened out with fever are highly expected to have an abnormal body temperature.

In its turn, Bardou *et al.* [9] announced the inclusion of mass screening for fever detection using a thermal camera in a university hospital in Southern France. They argue that infrared thermal cameras are a reliable and fast way to detect fever in clinical environments. However, such equipment must be calibrated to adjust its thermal sensitivity to the on-site room temperature to achieve greater accuracy.

Recently, McConeghy *et al.* [10] performed two retrospective cohort studies to determine the best temperature threshold for fever detection in veterans living in nursing homes. They found that a temperature threshold of 37.2ºC has better sensitivity for predicting positive COVID-19 patients when compared with the pré-established limit of 38ºC. Moreover, they also conclude that temperature screening alone is insufficient to predict positive testing for COVID-19 among residents.

In the same line of argument, a recent clinical evidence assessment [11] concluded that there was insufficient evidence to suggest that contact-less infrared temperature screening is effective for detecting people having COVID-19. Moreover, this review of the evidence points out several factors affecting the performance of such devices, namely, the environmental temperature and the need for calibration, the operating distance from individuals being tested, the use of medications to suppress abnormal body temperature, the physical activity, and the sensitivity of the infrared sensor.

The lessons learned from the previous discussion help us with the design of our study. Therefore, in our work, we are interested in assessing the performance of low-cost infrared thermography systems to detect elevated body temperature instead of identifying individuals testing positive for COVID-19. Moreover, we found that infrared devices must be calibrated for each environment, the temperature threshold for fever should be adjusted according to the population and environment characteristics, and the distance from the sensor must be well established. Finally, medication to suppress fever and people's physical activity must be taken into account.

III. ADOPTED METHODOLOGY

This section will describe the methodology that was defined and implemented for the evaluation of the sensors, as well as a description of the sensors themselves and their characteristics.

A. Region-of-Interest Definition

As the sensor's Field of View (FoV) covers an area much larger than the body of the subject to be screened, there was a need for defining shorter areas that limit the number of background pixels — selected after the detection of the highest temperature pixel — from now on defined as Region of Interest (RoI). Thus, the RoI has been defined using a square shape of approximately the size of the head of a person, considering the FoV of the camera when the subject was at a distance of 1 m. This way, the RoI temperature can be computed using distinct weights for the RoI pixels, c.f. Fig. 1.
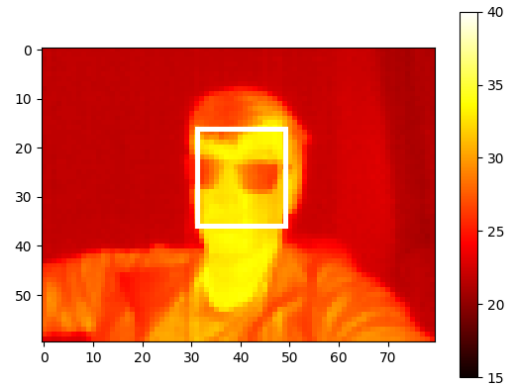

Fig. 1. Defining the Region of Interest (RoI). Image captured with a FLIR Lepton 2.5 [12]. Temperature scale is in degrees Celcius (ºC).

B. Computing RoI temperature

Four methods have been tested to compute the temperature inside the RoI, and have been compared with the reference camera (FLIR E54 [13]). The aim was to evaluate accuracy in the detection of elevated body temperature events, and not to replace traditional temperature screening methods typically used to measure absolute temperatures. The evaluated methods rely on data aggregation within the RoI, which also helps to reduce the impact of artifacts and noise during screening. The four evaluated methods for computing the RoI temperature were the following:

- **Method A**: arithmetic average considering all the pixels inside the RoI;

- **Method B**: weighted average consisting of the central pixel in the RoI weighted with 50%, and the remaining pixels equally weighted with the remaining 50%.

- **Method C**: arithmetic average among half of the pixels of the RoI with higher temperatures;
- **Method D**: arithmetic average among all the pixels with a deviation no higher than 2ºC from the highest temperature pixel.

C. Evaluation Procedure

After defining the RoI and the methods evaluated for computing the RoI temperature, an evaluation procedure — as can be observed in the experimental apparatus depicted in Fig. 2 — based on the recommendations of FDA [14] has been put forward:

1) The thermal sensors were set up and the reference camera (FLIR E54) was configured to operate in the screening mode (Emissivity set to 0.98). Then, the camera was left active for at least 15 minutes;
2) The subject was placed at 1 meter from the thermal sensors;
3) The ambient temperature and humidity have been registered with a hygrometer;
4) The temperature has been computed based on the RoI data using the methods previously defined;
5) The experiment was repeated multiple times.
6) The results have been evaluated from the multiple experiments based on statistics (average and standard deviation) and its evolution in time;
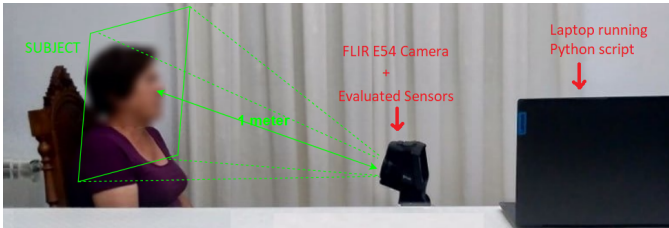

Fig. 2. Experimental setup, where the subject and the thermal camera have been placed at a distance of 1 m.

D. Characteristics of the evaluated IR sensors

Table I depicts the main characteristics of the reference camera (FLIR E54) used in the evaluation process and both IR sensors evaluated in this work. The MLX90640 sensor has a resolution of 32×24 pixels, resulting in a pixelated image and forcing larger areas over each pixel. The MLX90640 was connected to a Raspberry Pi using the I2C standard. The Lepton 2.5 sensor has a resolution of 80×60 pixels, so the resulting image has a resolution more than two times higher which results in a more visually perceptible image when compared

with the MLX90640. The Lepton 2.5 was connected to the Raspberry Pi using the USB protocol. During the experiments, the FLIR E54 thermal camera was used as reference equipment due to its high accuracy of ±0.3ºC [13]. The FLIR E54 was connected to a personal computer using proprietary software, and all the processing has been performed using the Python programming language.

TABLE I
REFERENCE CAMERA AND EVALUATED SENSORS CHARACTERISTICS.

Sensor	Resolution	FOV	Range(°C)	Price
FLIR E54 [13]	320×240	24º	-20ºC to 650ºC	4999€
MLX90640 [15]	32×24	55º	-40ºC to 300ºC	45€
Lepton 2.5 [12]	80×60	50º	-10ºC to 140ºC	130€

IV. RESULTS

A. IR Sensors Evaluation

The evaluation of both sensors has been performed during the same experiment through a Python script. The data has been collected as a thermal array from each sensor, and then transformed into a thermal matrix, before applying a specific RoI temperature computation method. Then a payload is created, which consists of a timestamp and the specific RoI temperature.

The different resolutions of the sensors under evaluation resulted in distinct RoI sizes. For the same FoV, the MLX90640 sensor RoI was set to an area of 7×7 pixels, resulting in a total of 49 pixels. For the Lepton 2.5 sensor, the RoI was set to 15×15, resulting in a total of 225 pixels. Figure 4 depicts the Method C visual aid used for computing the temperature within the RoI.
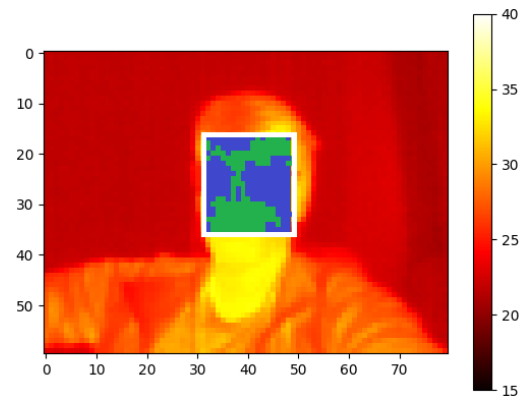

Fig. 4. Method C visual aid. Image captured with the FLIR Lepton 2.5 [12]. Temperature scale in degrees Celcius (ºC).
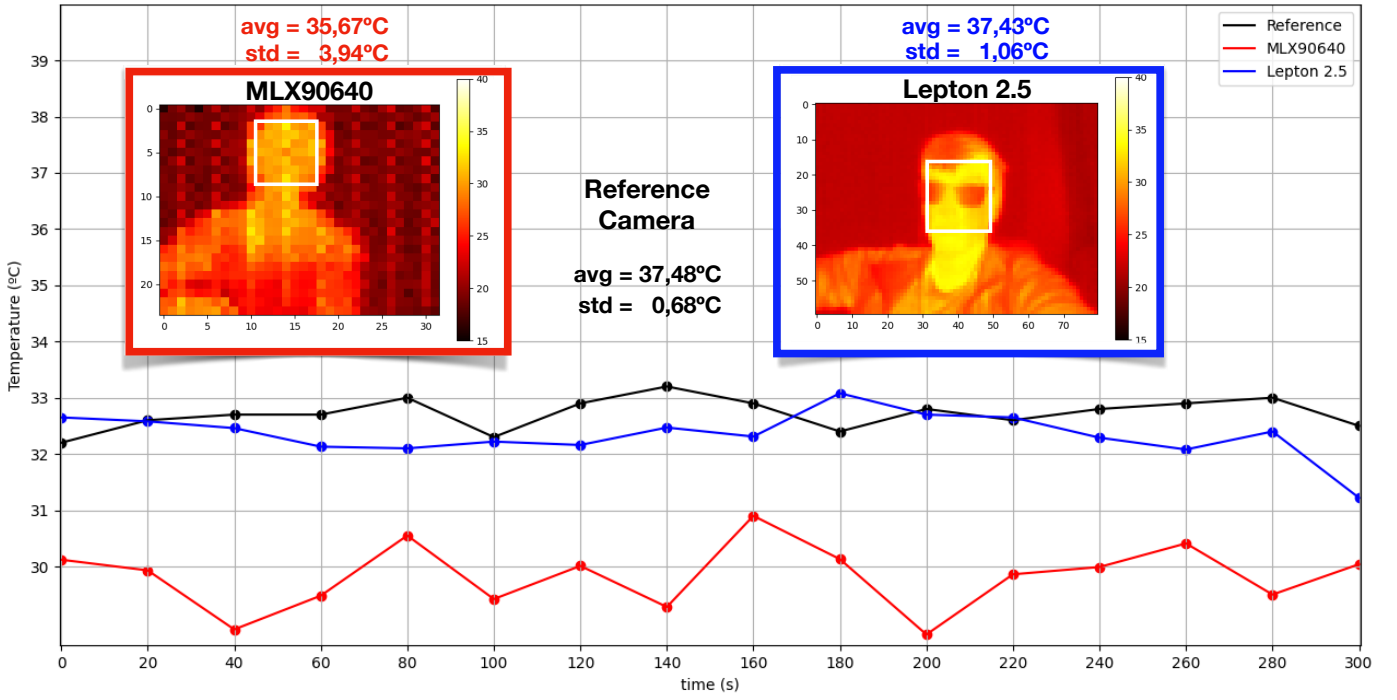
Fig. 3. Comparison of the IR sensors evaluated using the Method C under controlled conditions. Temperature scale in degrees Celcius (ºC).

The experiment was performed during 5 minutes and both evaluated sensors and the reference camera (FLIR E54) have been configured to capture data in sync, cf. the experimental apparatus presented in Fig. 2. Table II compiles the results obtained with the four methods evaluated to compute the RoI temperature. Method C was the one that presented the lower standard deviation throughout the experiment, and as such, was the one chosen to be used for detecting elevated body temperature events. During the experiments, the room temperature and humidity were registered with 21.6ºC and 55%, respectively. During the experiment, the average temperature, and the standard deviation, obtained with and reference camera (FLIR E54) were 37.48ºC and 0.68ºC, respectively.

TABLE II
WEIGHTED RoI TEMPERATURE USING THE FOUR METHODS.

Sensor		Method			
		A	B	C	D
MLX90640	Mean	34.26ºC	35.31ºC	35.67ºC	35.73ºC
	Std	3.94ºC	2.75ºC	2.41ºC	3.68ºC
Lepton 2.5	Mean	36.60ºC	37.31ºC	37.43ºC	36.03ºC
	Std	1.06ºC	0.98ºC	0.8ºC	1.68ºC

Figure 3 depicts the results obtained when using Method C for RoI temperature measurement with the reference camera (black line) and with both IR sensors under evaluation (red line — MLX90640; blue line — Lepton 2.5). The experiment was performed for 5 minutes upon controlled conditions. The distance from the sensors to the forehead of the subject was 1 meter, the recorded ambient temperature was 21.6ºC and relative humidity was 55%.

From the results observed in Figure 3, one can conclude that the Lepton 2.5 sensor can, not only detect temperature variations with relative correctness but also may be used to detect temperature when the need for the accuracy is not below ±1ºC error.

Moreover, the Python script can detect if the hardware is faulty or not present, raise exceptions to help with troubleshooting of the hardware, and also validates the format of the data coming from the sensors.

B. Detecting Elevated Body Temperature Events

Elevated body temperature events were defined for raising alerts to the caretakers, these consist of detecting continuous temperature increase over time or the detection of high temperatures in subjects which are triggered when the temperature goes over a preset threshold. The setup and procedure for testing these alerts consisted in using the same setup and methodology as before but forcing a raise of the subject's temperature using a towel dampened with water at 42ºC. The
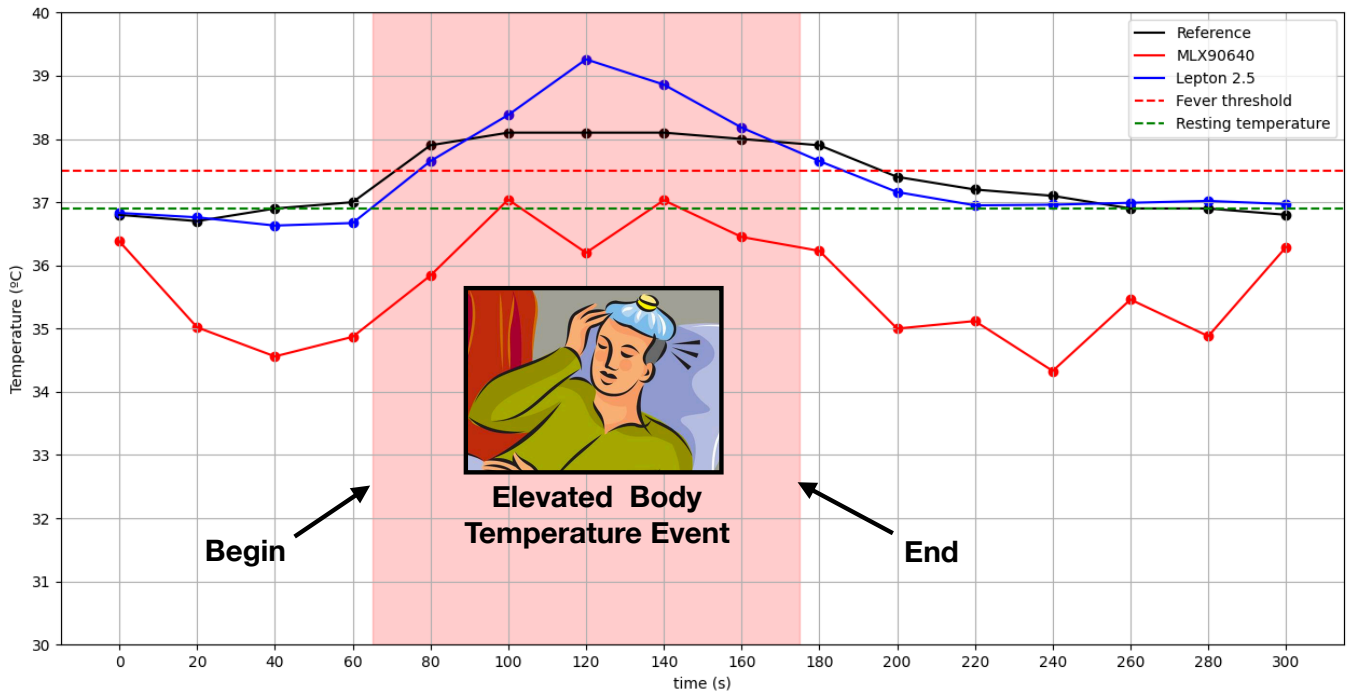
Fig. 5. Induced elevated body temperature event.

measurements were taken as before but the towel was put on the subject's forehead at the 65th second and taken out at the 175th.

Figure 5 depicts the results obtained after physically simulating an elevated temperature event. In this case, it can be seen that all the sensors managed to detect the elevation of the subjects' temperature.

The MLX90640 sensor is capable of detecting thermal variations over time, though in the situation that this setup is to be implemented, however, the reliability and accuracy of this sensor are not appropriate for the use case under study.

On the other hand, when using the Lepton 2.5 sensor we can follow the increases and decreases screened with the reference camera. It also presents values much closer to the reference ones allowing the sensor to be much more accurate and viable in the context of this project.

V. CONCLUSIONS AND FUTURE WORK

In this work, we present the methodology adopted for the assessment of low-cost infrared thermography systems for medical screening in nursing homes, where these sensors can play a crucial role as an adjunctive diagnostic screening tool for caregivers and health professionals, allowing the continuous acquisition of temperature and therefore contribute to the early detection of elevated body temperature events,

without aiming to replace conventional diagnostic methods. Two low-cost sensors have been evaluated, the MLX90640 and the FLIR Lepton 2.5, and as a result, we observed that the latter can fit the application under study, which aims to detect elevated body temperature events.

As future work, we will focus on the automatic detection of body parts, to automatically identify the subject's body in various RoI, i.e., head, torso, and arms. Moreover, in the case that the sensor FoV covers the whole bedside, we aim to implement a set of alerts that can anticipate possible falls, that may occur when the person is moving towards the bed's edge.

REFERENCES

[1] F. Niklaus, C. Vieider, and H. Jakobsen, "Mems-based uncooled infrared bolometer arrays: A review," in *MEMS/MOEMS technologies and applications III*, International Society for Optics and Photonics, vol. 6836, 2008, p. 68360D.

[2] O. Breitenstein, W. Warta, and M. C. Schubert, "Introduction," in *Lock-in Thermography: Basics and Use for Evaluating Electronic Devices and Materials*. Cham: Springer International Publishing, 2018, pp. 1–6, ISBN: 978-3-319-99825-1. DOI: 10.1007/978-3-319-99825-1_1.

[3] B. B. Lahiri, S. Bagavathiappan, B. Raj, and J. Philip, "Infrared thermography for detection of diabetic neuropathy and vascular disorder," in *Application of Infrared to Biomedical Sciences*, E. Y. Ng and M. Etehadtavakol, Eds. Singapore: Springer Singapore, 2017, pp. 217–247. DOI: 10.1007/978-981-10-3147-2_13.

[4] J. Pauk, A. Wasilewska, and M. Ihnatouski, "Infrared thermography sensor for disease activity detection in rheumatoid arthritis patients," *Sensors (Basel, Switzerland)*, vol. 19, no. 16, p. 3444, Aug. 2019, s19163444[PII], ISSN: 1424-8220. DOI: 10.3390/s19163444.

[5] L. Shu, W. Bai, T. Shimada, Z. Ying, S. Li, and N. Sugita, "Thermographic assessment of heat-induced cellular damage during orthopedic surgery," *Medical Engineering and Physics*, vol. 83, pp. 100–105, 2020, ISSN: 1350-4533. DOI: 10.1016/j.medengphy.2020.05.014.

[6] M. Soroko, R. Henklewski, H. Filipowski, and E. Jodkowska, "The effectiveness of thermographic analysis in equine orthopedics," *Journal of Equine Veterinary Science*, vol. 33, no. 9, pp. 760–762, 2013, ISSN: 0737-0806. DOI: 10.1016/j.jevs.2012.11.009.

[7] D. Perpetuini, C. Filippini, D. Cardone, and A. Merla, "An overview of thermal infrared imaging-based screenings during pandemic emergencies," *International Journal of Environmental Research and Public Health*, vol. 18, no. 6, 2021. DOI: 10.3390/ijerph18063286.

[8] A. L. Hewlett, A. C. Kalil, R. A. Strum, W. G. Zeger, and P. W. Smith, "Evaluation of an infrared thermal detection system for fever recognition during the h1n1 influenza pandemic," *Infection Control amp; Hospital Epidemiology*, vol. 32, no. 5, pp. 504–506, 2011. DOI: 10.1086/659404.

[9] M. Bardou, P. Seng, L. Meddeb, J. Gaudart, E. Honnorat, and A. Stein, "Modern approach to infectious disease management using infrared thermal camera scanning for fever in healthcare settings.," *The Journal of infection*, vol. 74 1, pp. 95–97, 2017.

[10] K. W. McConeghy, E. White, O. A. Panagiotou, C. Santostefano, C. Halladay, R. A. Feifer, C. Blackman, J. L. Rudolph, V. Mor, and S. Gravenstein, "Temperature screening for sars-cov-2 in nursing homes: Evidence from two national cohorts," *Journal of the American Geriatrics Society*, vol. 68, no. 12, pp. 2716–2720, 2020. DOI: 10.1111/jgs.16876.

[11] ECRI, "Infrared temperature screening to identify potentially infected staff or visitors presenting to healthcare facilities during infectious disease outbreaks," 2020. [Online]. Available: https://api.semanticscholar.org/CorpusID:214666658.

[12] FLIR, "Lepton 2.5 Datasheet." [Online]. Available: https://lepton.flir.com/wp-content/uploads/2015/06/lepton-2pt5-datasheet-04195.pdf, (accessed: 11.08.2021).

[13] Teledyne FLIR, "FLIR E54." [Online]. Available: https://www.flir.com/products/e54/, (accessed: 11.08.2021).

[14] U. S. Food and D. A. (FDA), "Thermal imaging systems (infrared thermographic systems / thermal imaging cameras)," 2021. [Online]. Available: https://www.fda.gov/medical-devices/general-hospital-devices-and-supplies/thermal-imaging-systems-infrared-thermographic-systems-thermal-imaging-cameras, (accessed: 07.08.2021).

[15] Melexis, "MLX90640 Datasheet." [Online]. Available: https://www.melexis.com/en/documents/documentation/datasheets/datasheet-mlx90640, (accessed: 11.08.2021).